Molecular characterization of a prokaryotic polypeptide sequence that catalyzes Au crystal formation

John L. Kulp III,[a] **Mehmet Sarikaya**[b] **and John Spencer Evans***[a]

[a]*Laboratory for Chemical Physics, New York University, 345 E. 24th Street, New York, New York, 10010, USA. E-mail: jse1@nyu.edu*
[b]*Department of Materials Science and Engineering, University of Washington, Seattle, Washington 98105, USA*

The gold crystal-forming *E. coli* polypeptide sequence, MHGKTQATSGTIQS, is one of several polypeptide sequences that interacts with gold interfaces and catalyzes the formation of Au crystals in solution, with nucleated Au crystals preferentially featuring the (111) interface. To date, there have been no experimental studies which explore the structure of *E. coli*-expressed gold binding proteins or the binding of Au(III) ions by these polypeptides. In this present report, multidisciplinary approaches were applied to the 42-AA gold binding protein-1 (GBP-1/42) and to a model polypeptide representing the 14-AA integral repeat of this protein (GBP-1/14). CD and NMR spectroscopy indicate that neither the integral repeat nor the GBP-1 protein adopt folded structures in the apo form or in the presence of Au(III) ions; the integral repeat adopts a random coil-extended structure conformation [*i.e.*, (*MHGKTQA*)*random coil*–(*TSGTIQS*)*extended*] and the GBP-1 protein appears to be similarly structured. These features are inconsistent with a templating structure. Mass spectrometry experiments indicate that the integral repeat binds up to two Au(III) ions per polypeptide molecule, and ¹H NMR ROESY experiments pinpoint the interaction of Au(III) within two sites: the -QAT- region of the integral repeat MHGKTQATSGTIQS sequence, and, at the negatively charged C-terminus of this sequence. Collectively, our findings support the hypothesis that GBP-1 does not catalyze Au crystal formation *via* a templating mechanism; rather, the open, unfolded structure of this protein, combined with the presence of accessible proton donor/acceptor amino acids (Ser, Thr, Lys, Gln, His) most likely play a role in Au crystal formation in solution and may also explain the interactive nature of this polypeptide with Au interfaces.

Introduction

The use of combinatorially-selected polypeptides that recognize and interact with non-natural inorganic substrates such as metals,[1–5] ceramics,[6–8] and semiconductors[9,10] has emerged as a new tool for nanoscale technologies that include the morphogenesis of small particles,[1,2,4] the rate control of crystal formation,[4] and assembly of semiconductors and ordered arrays of metal particles.[9,10] To date, these polypeptide sequences are generated genetically *via* substrate screening of phage display libraries[6–10] or bacterial[1–5] exposure against various inorganic solids, with subsequent washing, screening, and sequencing procedures for identifying material-specific, high affinity polypeptide sequences. This complex and dynamic biomimetic approach to nanomaterial design mimics the protein-based catalysis, recognition, and binding mechanism found within the biomineralization process, where organisms have long employed proteins to control and modify the formation of inorganic solids in solution.[11–17] Yet, little is known about the sequence–structure relationships involved in genetically engineered peptides which interact with or catalyze the formation of inorganic solids.

Perhaps the best characterized series of inorganic-interaction prokaryotic polypeptides are the *E. coli*-specific metal binding polypeptide sequences.[1–5] One of these sequences, gold binding protein-1 (GBP-1, 42 AA, [MHGKTQATSGTIQS]$_n$, where n = 3, 5, 7), was developed in an *E. coli* cell-surface display system in the presence of exposed gold metal surfaces.[1–4] This protein has an interesting dual character: GBP-1 has been shown to interact with exposed gold crystal interfaces under high ionic strength conditions;[2,3] and, the -KTQATS- sequence has been shown to participate in the nucleation of gold crystals

from Au(III) ions in solution,[3,4] with the nucleated crystals predominantly featuring the {111} interface, similar to what is observed for Au crystals formed in the presence of boiling citric acid.[4] However, the molecular mechanisms by which GBP-1 recognizes and binds to Au solid interfaces and/or catalyzes the formation of Au crystals are not understood.

If we wish to understand the underlying mechanisms involved in -KTQATS- mediated Au crystal formation, then we need to address some fundamental issues. Given that rigid, organized structures are typically associated with a molecular nucleation template,[18–22] it is possible that the GBP-1 adopts a fold or conformation that facilitates Au(III) ion assembly on the protein surface and subsequently triggers a templating mechanism. Alternatively, the -KTQATS- sequence may influence Au crystal formation *via* a non-templating mechanism, such as the proposed acid-catalyzed mechanism, wherein the GBP protein regulates the local pH or proton concentration in the vicinity of Au clusters.[4] In that case, it is plausible that Au(III) interactions with a specific GBP-1 conformation influence the acid-catalyzed Au(III) → Au crystal formation process in some manner. In either scenario, there is a need to determine the site of Au(III) interaction within the -KTQATS- sequence, and, deduce the -KTQATS- and GBP-1 structure in the solution state if we are to unravel the protein-mediated Au crystal catalysis process and eventually probe GBP-1–Au crystal interactions in the solid-state.

Thus, the issues of polypeptide conformation, identification of Au(III)–-KTQATS-interactions, and the potential for Au(III)-induced GBP-1 conformational change become the initial focus of our research efforts. In this report, we address the issue of GBP-1 and -KTQATS- solution structure and the interaction of Au(III) with -KTQATS- and GBP-1 *via*

multidisciplinary studies (NMR, CD, mass spectrometry) of the integral GBP-1 sequence, MHGKTQATSGTIQS (denoted as GBP-1/14), and the 42 AA, $n = 3$ (triple repeat) version of the GBP-1 protein (denoted as GBP-1/42). Both GBP-/14 and GBP-1/42 were utilized in parallel studies to verify if either polypeptide possesses conformational preferences in the apo-state and/or undergoes conformational rearrangement in the presence of Au(III). Since GBP-1/42 induces Au(III) → Au(s) precipitation and also experiences aggregation in the presence of Au(III),[4] thorough solution-based experimentation with this version is difficult. Hence, the single repeat version GBP-1/14, which does not exhibit Au(III) induced aggregation, was primarily employed in our study to verify Au(III)–peptide interactions and Au(III) site binding within the -KTQATS- sequence. As shown in this report, we find that both the -KTQATS- and GBP-1 possess features that are inconsistent with the notion of a molecular template: both polypeptides adopt unfolded, conformationally labile structures in the presence and absence of Au(III). Moreover, we identify that the -QAT- sequence within the MHGKTQATSGTIQS repeat is a plausible site for Au(III) interaction, and we believe that the combined attributes of unfolded structure and Au(III) interaction capability are essential for Au crystal formation.

Materials and methods

GBP-1/14, GBP-1/42 synthesis and purification

Purified 14- and 42-mer free termini polypeptides were synthesized by United Biochemical Research, Inc. (Seattle, WA) using an Applied Biosystems 431A Peptide Synthesizer, NovaSyn TGA resin (Novabiochem, San Diego, CA), and N$^\alpha$-L-FMOC-amino acids.[17,23] Typical peptide synthesis runs were carried out at the 50 μmol level. The completed peptides were deprotected and cleaved (reaction time = 3 h, at 25 °C) from the resin using a cleavage cocktail [15 mL (g resin)$^{-1}$] containing 90% v/v TFA, 2.5% v/v water, 2.5% v/v ethanedithiol, 2.5% v/v phenol, and 2.5% v/v thioanisole;[17,23] the thiol scavengers were utilized to enhance Gln trityl protecting group removal and prevent reaction of Met sidechain sulfur atom with the trityl-carbocation generated during cleavage. The reaction mixtures were filtered under reduced pressure. The crude peptides, free of sidechain protection, were separately dissolved in deionized distilled water, extracted three times with diethyl ether, and then concentrated and lyophilized. Peptide purification involved the use of a C8 reverse phase high performance liquid chromatography (HPLC) column, using 0.1% TFA/water mobile phase and eluting with an acetonitrile/0.8% TFA/water linear gradient (0% to 50% solvent B in 40 minutes). Peptide elution was monitored at 214 nm. Typically, a 50 μmol synthesis of each peptide yielded 6 mg of GBP-1/14 and 16 mg of GBP-1/42 dry mass >95% in purity and free of sidechain protection. The experimental molecular weight for the free termini 14- and 42-mer polypeptides were determined via matrix-assisted laser desorption-ionization time-of-flight (MALDI/TOF) mass spectrometry to be 1447 Da and 4304 Da, in agreement with the theoretical molecular weight of 1446.5 Da and 4303.6 Da, respectively.

Mass spectrometry Au(III) binding studies

For (MALDI/TOF) studies, the GBP-1/14 peptide was dissolved in deionized distilled water to a final concentration of 100 μM. The matrix α-cyano-4-hydroxycinnamic acid (HCCA), AuCl$_3$ (99.99% purity), Tris-HCl , and acetonitrile (spectral grade, glass distilled) were purchased from Aldrich Chemicals. All aqueous solutions were prepared using deionized distilled water (metal ion content <1 ppb). Matrix solutions were prepared using a saturated solution of HCCA in 30%/70% v/v acetonitrile : water. Apo samples for MALDI/ TOF were prepared as follows. First, 4 μL of peptide stock solution, 4 μL water, and 1 μL of 300 mM Tris-HCl (pH 7.5) were vortexed. Next, 1 μL of the vortexed solution was added to 50 μL of matrix solution, followed by vortexing. Finally, 1 μL of this solution was applied to the MALDI probe grid and air dried at 25 °C. For metal ion : peptide samples, the same mixing procedure was utilized; however, 4 μL of metal ion stock solution was substituted for the water in the first mixing step, prior to the introduction of the 50 μL matrix solution, such that a 1 : 100 and 1 : 1000 GBP-1/14 : metal ion sample was created. Note that after final mixing, the pH of all samples was found to be in the range of 7.0–7.2. MALDI/TOF-MS experiments were performed on Bruker Daltonics delayed-extraction linear TOF spectrometer. All MALDI/TOF-MS spectra were acquired in positive ion mode by averaging 50 single shots. Internal mass calibration was obtained using the ProteoMass Peptide MALDI-MS Calibration Kit from Sigma Aldrich [Milwaukee, WI, USA; brandykinin fragment 1–7 (757.4 Da), angiotensin II (1046.5 Da), ACTH fragment 18–39 (2465.2 Da)].

For ion trap mass spectrometry, apo-GBP-1/14 was dissolved in deionized distilled water to a final concentration of 500 μM. For the GBP-1/14 : Au complex, an appropriate microliter volume of AuCl$_3$ stock solution was added to a parallel apo-peptide sample to create a metal ion : peptide ratio = 10 : 1, with the final peptide concentration = 500 μM. Peptide samples were run on an Agilent LC-MSD Trap-XCT Mass Spectrometer, and were individually injected at a rate of 10 μL min^{-1}, and mass spectrometer parameters included a positive ion polarity, dry temperature = 350 °C, and nebulizer setting of 50 psi.

CD spectrometry

For CD studies of the apo-form, GBP-1/14 and GBP-1/42 were dissolved in either 100 μM Na$_2$HPO$_4$, pH 7.6 or 100 μM NaH$_2$PO$_4$, pH 2.58 buffers, to a final concentration of 12 μM. For Au(III)–peptide binding studies, gold ion titrations of both polypeptides were performed using stoichiometric amounts of Au(III) (i.e., mole peptide : Au = 1 : 1, 1 : 2, 1 : 4 for GBP-1/14; 1 : 1, 1 : 3 for GBP-1/42). These titrations were performed by adding microliter volumes of 100 mM AuCl$_3$ stock solution (99.99%, Aldrich Chemicals) to either polypeptide (12 μM) in 100 μM Tris–HCl buffer, pH 7.5. CD spectra were obtained using an AVIV 60 CD spectrometer, running 60DS software version 4.1t. Peptide samples were scanned from 185 to 260 nm at 5 °C, using 1 nm bandwidth and a scan rate of 1 nm/sec, with appropriate background buffer subtraction performed. These experiments were performed at 5 °C to slow down the conformational lability or exchange within the GBP-1/14 and GBP-1/42 polypeptides.[23] The spectrometer was previously calibrated with d$_{10}$-camphorsulfonic acid. A total of 3 scans were acquired for each peptide sample. Mean residue ellipticity [θ_M] is expressed in deg cm^2 dmol^{-1} per mole peptide.

NMR spectroscopy

For NMR studies of the apo-form, 1.4 mM GBP-1/14 and 850 μM GBP-1/42 samples were created using deionized distilled water, with 10% v/v deuterium oxide (99.9% atom D, Cambridge Isotope Labs) and 10 μM d$_4$-TSP added. The pH was adjusted to 7.6 using NaOH; the peptide provided the buffering capacity. At these polypeptide concentrations turbidity measurements at 380 nm revealed no evidence of peptide aggregation; this also was confirmed by analyses of NMR proton chemical shifts and linewidths and the absence of long-range d$_{sc–sc}$ NOE connectivities. For NMR studies of the 1 : 1 GBP-1/14 : Au(III) complex, we utilized a 1.4 mM GBP-1/14 polypeptide sample in 90% H$_2$O/10% D$_2$O, to which

an equimolar amount of $AuCl_3$ stock solution was added. After mixing, the pH was checked and adjusted to pH 7.6 using NaOH/HCl. NMR experiments were performed on Varian UNITY 500 and Bruker AVANCE-500 z-PFG spectrometers. With the exception of the amide temperature shift experiments, all reported NMR experiments were conducted at 278 K in order to slow down conformational exchange within the polypeptides. Proton scalar coupling assignments were obtained using 2-D pulsed-field-gradient (PFG) "clean" total correlation (TOCSY) experiments.[23,24] Water suppression was achieved using either excitation sculpting, WATERGATE, or 3-9-19 z-axis PFG gradient schemes. Proton sequential assignments and NOEs were obtained using z-PFG NOESY and rotating-frame nuclear Overhauser (ROESY) experiments[23,24] (t_m = 50 ms to 200 ms). $^3J_{NH-CH_\alpha}$ values were determined for the 14-mer using spectral processing methods which permit coupling constant measurements from TOCSY/ROESY/NOESY spectra.[25] The crosspeak linewidths were not significantly affected by line broadening as evidenced by comparisons of spectra obtained at 5 °C and 20 °C (data not shown). Using PFG TOCSY or ROESY experiments at 278, 283, 288, 293, 298, 303, and 308 K, amide proton temperature coefficients for GBP-1/14 were determined from the slope of the temperature versus amide proton chemical shift curves for each residue.[23] Temperature gradients are expressed in units of ppb K^{-1} with a negative sign indicating an upfield shift upon warming.[23] Temperature calibration of the VT unit was determined prior to experimentation using neat methanol over a temperature range of 273 to 320 K. NMR data were processed using FELIX2000 (Acelerys, Inc.) or Bruker XWINNMR software. Relevant NMR acquisition and processing parameters are provided in the figure legends.

Results

Mass spectrometry Au(III)–polypeptide binding experiments

We employed MALDI/TOF and ion-trap mass spectrometry to detect GBP-1/14 : Au adduct species via the metal ion-induced mass shift method.[23,26,27] This approach has successfully determined the metal binding properties of polypeptides and deduced ion : peptide stoichiometries with high sensitivity.[23,26,27] In order to displace ubiquitous sodium ions which remain after peptide purification, and, to ensure sufficient peptide : metal ion complex formation, the mass shift method requires the use of a molar excess of metal ions (i.e., peptide : metal = 1 : 100 or greater for MALDI/TOF = 1 : 10 for ion trap).[23,26,27] Note that since neither technique is quantitative, we cannot provide information regarding peptide : metal ion affinities at this time. Using MALDI/TOF-MS, we observe the $[M + H^+ + H_2O]$, $[M - (H^+) + Na^+ + H_2O + H^+]$ and $[M - (H^+) + (Au^{3+})_n + H_2O + H^+]$ adduct species, where M = GBP-1/14 and n = 1 (Fig. 1A). Significant GBP-1/14 fragmentation was noted in the presence of Au(III) using the MALDI/TOF-MS method (Fig. 1A). Note also that, despite the use of mole excess of Au(III), peptide : Na^+ adducts persist as common species in MALDI/TOF–MS spectra for polypeptides possessing free α-carboxylate termini.[23] For comparison, the ion trap mass spectra of the 1 : 10 GBP-1/14 : Au(III) sample reveals the presence of a major adduct species, $[M + (Au^{3+})_n]$, where n = 2; note that the n = 1 adduct was not observed. From the ion trap and MALDI/TOF results, we conclude that the -KTQATS- containing GBP-1/14 peptide has the capability of interacting with Au(III) ions. Note that parallel MALDI/TOF-MS and ion trap experiments were conducted with GBP-1/42 in the presence of Au(III); however, these studies failed to detect any peptide : Au(III) adduct species, most likely as a result of Au(III)-induced GBP-1/42 aggregation.
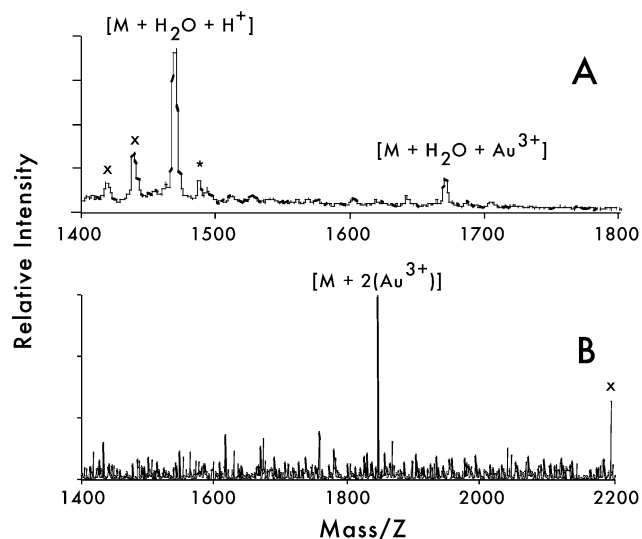

Fig. 1 (A) MALDI/TOF mass spectra of GBP-1/14 polypeptide in the presence of $AuCl_3$ (peptide : ion = 1 : 1000). Mass of Au(III) = 197 a.m.u.; mass of Na^+ = 23 a.m.u. Observed masses of MALDI/TOF adducts: $[M + H^+ + H_2O]$, 1465.6 Da experimental (1466 Da theoretical); $[M + Au^{3+} + H^+ + H_2O]$, 1664.05 Da experimental (1663 Da theoretical). Sodium ion–GBP-1/14 adducts are denoted by the "*" symbol. Peptide fragmentation adducts are denoted by the "X" symbol. (B) Ion trap mass spectra (positive ion mode) of GBP-1/14 in the presence of $AuCl_3$ (peptide : ion = 1 : 10). Observed mass of major singly charged $[M + (Au^{3+})_2]$ adduct = 1843.2 Da (1842.4 Da theoretical). In spectrum (B), "X" denotes unknown GBP-1/14 adduct species.

CD spectrometry of apo- and Au(III)-bound polypeptides

The far UV circular dichroism spectra of the apo-forms of GBP-1/14 and GBP-1/42 polypeptides reveal the presence of a broad π–π* absorption band centered near 198 nm at pH 7.6 (Fig. 2), indicating that the conformation of both polypeptides are similar to one another. Similar spectra were obtained at pH 2.6 (data not shown). The CD spectra of GBP-1/14 and GBP-1/42 are inconsistent with the presence of a β-hairpin structure, but are consistent for a conformationally-labile polypeptide consisting of random-coil in equilibria with other
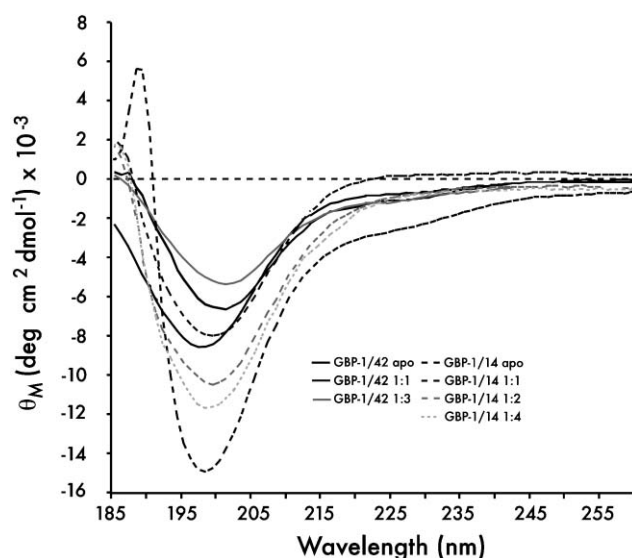

Fig. 2 Far UV CD spectra of apo-GBP-1/14 and GBP-1/42 polypeptides at pH 7.6, 5 °C, sodium phosphate buffer, and, in the presence of $AuCl_3$, pH 7.6 Tris-HCl buffer, 5 °C. Peptide : Au(III) stoichiometries are given in the figure. Note that due to Au(III) – induced precipitation of GBP-1/42, stoichiometries higher than 1 : 3 peptide : Au(III) could not be analyzed.
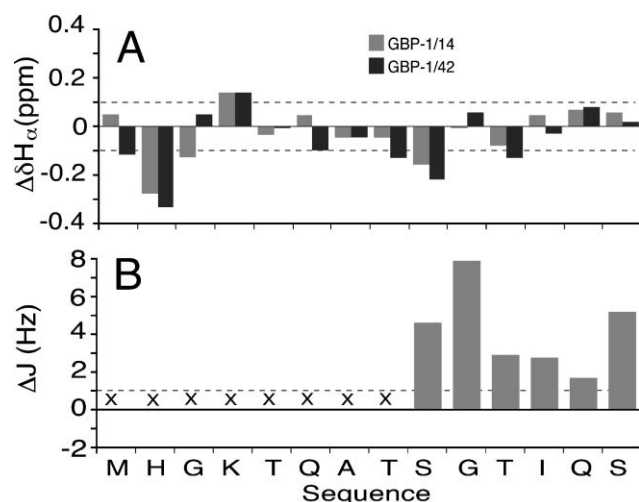
Fig. 3 (A) $\Delta\delta H_\alpha$ values ($\delta H_{\alpha, \text{observed}} - \delta H_{\alpha, \text{random coil}}$) obtained for GBP-1/14 and GBP-1/42 in 100 μM Na_2HPO_4, pH 7.6, 90% H_2O/10% D_2O, 278 K. Negative values represent upfield shifts, positive values represent downfield shifts. No corrections have been made for terminal residue effects; however, corrected CH_α chemical shift values were utilized for A7 and Q6 nearest neighbor effects.[36,37] Proton chemical shifts were referenced from internal d$_4$-TSP. (B) Calculated difference (ΔJ, $^3J_{\text{observed}} - ^3J_{\text{random coil}}$) between experimental and random coil $^3J_{\text{NH-CH}_\alpha}$ values for GBP-1/14, pH 7.6, 90% H_2O/10% D_2O, 278 K. Note that several ΔJ values could not be quantitated due to crosspeak overlap (indicated by "X" symbol). In both graphs, the dashed line represents the random coil threshold value (*i.e.*, $\Delta\delta H_\alpha < 0.1$ ppm; $\Delta J > 1$ Hz).

secondary structures, such as loop, turn, extended, polyproline Type II, or β-strand.[17,23,28–30]

With the stoichiometric addition of AuCl$_3$, band intensity changes are noted for GBP-1/14, but no significant wavelength shifts are observed for the π–π* band (Fig. 2), nor are any additional adsorption bands observed. This data indicates that Au(III) interaction does not induce α-helix or β-strand formation within -KTQATS- containing GBP-1/14.[17,23,28-30] Parallel AuCl$_3$ titrations were also performed on GBP-1/42; here, at 1 : 1 and 1 : 3 peptide : Au(III) stoichiometries, we observe a small wavelength shift (198 nm to 202 nm) in the π–π* band for GBP-1/42, but we do not observe the appearance of additional bands associated with α-helix or β-strand conformations. Note that at GBP-1/42 : Au(III) stoichiometries > 1 : 3, we observed the appearance of Au–peptide precipitates; thus there is no additional CD spectral information beyond this stoichiometric level.

Collectively, our CD data indicates that the GBP-1/42 protein does not fold into a stable secondary structure in the presence of Au(III), but does experience a detectable shift in conformational equilibria compared to the apo-state. *Thus, at neutral and low pH both the GBP-1/14 and GBP-1/42 polypeptides adopt an unfolded structure consisting of random coil conformation in equilibrium with other secondary structures. Furthermore, the addition of Au(III) ion does not significantly affect the global conformation of either the integral tandem repeat or the GBP-1 protein, i.e., both polypeptides persist as conformationally labile, unfolded species.* Thus, unlike other metallopolypeptides,[31–33] the GBP-1 protein and the -KTQATS- sequence do not experience significant metal ion-induced structural rearrangement.

NMR studies of apo-GBP-1/14

Based upon the strategy utilized in previous studies of multiple tandem repeat polypeptides,[34] we initially determine the structure of the single repeat form, and compare this to the overlapped NMR dataset obtained for the multiple repeat form. This allows us to infer whether the tandem repeats within the larger polypeptide adopt the structure of the single repeat.[34] For the single repeat, proton conformational shifts ($\Delta\delta H_\alpha$)[23,35–37] and ΔJ values,[23,38,39] were calculated (Fig. 3; note that ^1H NMR chemical shifts obtained for GBP-1/14 are presented in Table 1). Residues H2, G3, K4, and S9 exhibit $\Delta\delta H_\alpha > 0.1$ ppm, indicating that these residues exhibit significant deviation from random coil database values.[23,35–37] However, the majority of residues possess $\Delta\delta H_\alpha$ values < 0.1 ppm, suggesting the presence of a random coil state.[23,35–37] For those residues where $^3J_{\text{NH-CH}_\alpha}$ couplings could be unambiguously determined, we observe $+\Delta J$ values > 1 Hz for S9, G10, T11, I12, Q13, and S14 (Fig. 3). In general, ΔJ values > 1 Hz indicate significant deviation from random coil structure; (+) ΔJ values are typically indicative of β-strand conformation, (−) ΔJ values are representative of α-helix conformation, and ΔJ values for a β-turn can be either (+) or (−).[38,39] Thus, the $\Delta\delta H_\alpha$ and ΔJ values support the findings of the CD experiments, *i.e.*, the GBP-1/14 single repeat sequence adopts an unfolded conformation that possesses both random coil and non-random coil structural aspects, with the -SGTIQS- sequence region exhibiting deviation from random coil structure.

Quantitative sequence-specific NMR parameters obtained for GBP-1/14 (Figs. 4 and 5) reveals three traits that are uncharacteristic of folded polypeptide sequences such as α-helix, β-sheet, β-turn, or β-hairpin:[23,40–44] (1) An absence

Table 1 500 MHz Proton chemical shifts (ppm, at 278 K) for GBP-1/14 pH 7.6, 90% water/10% D_2O

Residue	NH	CH_α	CH_β	CH_γ	CH_δ	CH_ε	Ring H	Sidechain NH	$^3J_{\text{NH-CH}_\alpha}$/Hz
M1	8.73	4.37	1.97	2.37					—
H2	8.58	4.32	N/O				7.99	N/O	—
G3	8.62	3.86							18.2
K4	8.41	4.37	1.73, 1.81	1.4	1.63	2.94			—
T5	8.34	4.34	4.24	1.16					18.2
Q6	8.63	4.38	1.98, 2.06	2.34				7.34	—
A7	8.41	4.3	1.45						—
T8	8.38	4.33	4.15	1.16					—
S9	8.25	4.23	3.8						12.2
G10	8.6	3.98							14.1
T11	8.2	4.3	4.1	1.13					11.3
I12	8.45	4.13	1.8	1.15, 1.45	0.85				11
Q13	8.7	4.36	1.96	2.08	2.34			7.34	9.7
S14	8.48	4.43	3.86						12.8

^{a} The proton assignments were obtained from analyses of PFG-TOCSY and ROESY experiments. Diastereotopic protons are separated by commas. Proton chemical shifts are referenced from internal d$_4$-TSP. N/O = not observed. ^3J coupling constants were determined using z-PFG-TOCSY/ROESY experiments and spectral processing methods that permit coupling constant measurements from TOCSY and ROESY/NOESY spectra (estimated experimental error, ±0.9 Hz).[23] Dashed line indicates that coupling constants could not be determined due to crosspeak overlap.
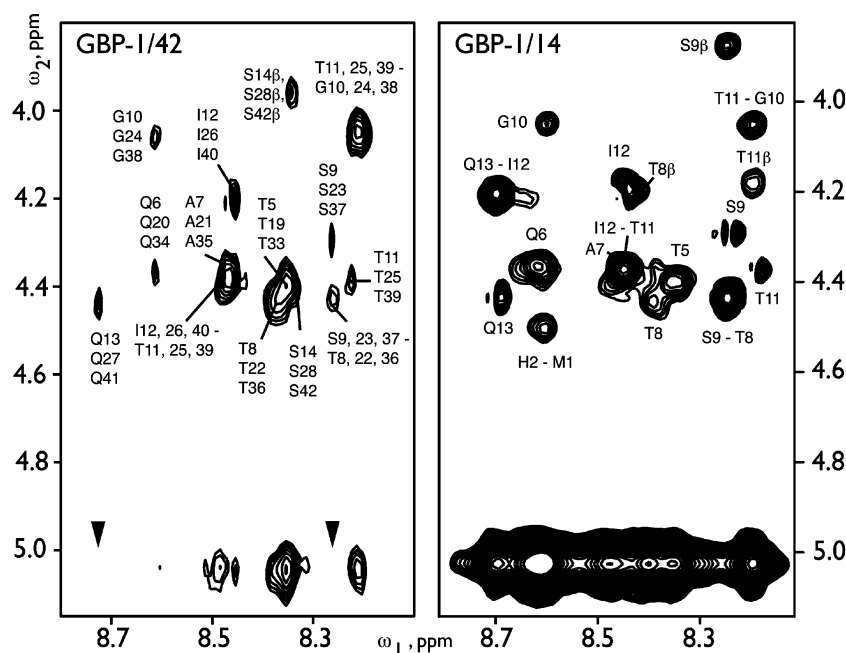
Fig. 4 PFG-ROESY (GBP-1/14) and NOESY (GBP-1/42) spectra for gold binding polypeptides in 100 µM Na_2HPO_4, pH 7.6, 90% H_2O/10% D_2O, 278 K. Acquisition parameters for GBP-1/14 included a relaxation delay of 1 s, spectral window = 5200 Hz, "hard" 90° = 8.7 µs, "hard" 180° = 17.4 µs; "soft" selective 180° = 3.2 ms; 256 transients per experiment were acquired; 2048 and 512 complex points were collected in t_1 and t_2, respectively. The carrier is centered on the water resonance. The t_m or mixing time for ROESY (compensated spinlock 180° pulse train) experiments was 200 ms. For GBP-1/42, the spectral window = 5123 Hz, "hard" 90° = 7.3 µs, "hard" 180° = 14.6 µs, with other parameters identical to those reported for GBP-1/14. The corresponding t_m for the GBP-1/42 NOESY experiment was 150 ms. Z-Gradient parameters: G_1 = 14 G cm^{-1}, G_2 = 6 G cm^{-1}, each with a duration of 1 ms with 500 µs stabilization time. The hypercomplex phase-sensitive method was utilized for processing both 2-D spectra, with zero-filling in the ω_2 dimension. Proton chemical shifts are referenced from internal d$_4$-TSP. In the GBP-1/42 spectra, arrows denote missing NH–solvent NOE connectivities.

of long-range backbone NOEs (*i.e.*, > i + 1) (Figs. 4 and 5), indicating that the single repeat does not possess either α-helix or β-hairpin structure;[40–44] (2) An absence of sequential $d_{NN(i, i + 1)}$ NOEs (Figs. 4 and 5), which is consistent with either NH–NH interproton distances > 5.5 Å (*i.e.*, extended structure) or conformational exchange due to the presence of random coil states;[40–44] and (3) No evidence for backbone NH protons shielding from solvent exchange, as witnessed by the large, negative amide temperature shift coefficient (ATC) values obtained for all residues in this sequence (all values > −9.9 ppb K^{-1}, data not shown)[23,45] and the detection of ROESY solvent–amide proton exchange cross-peaks for all residues within the 14-mer sequence (Fig. 4). Note that random coil structures typically exhibit ATC values ranging from −6.6 to −9.0 ppb K^{-1}.[23,45] The ATC values and ROESY water exchange spectra are consistent with the absence of intrastrand backbone hydrogen bonding, and/or the absence of polypeptide folding that would protect NH backbone sites from solvent exchange.[23,45]

Thus, having ruled out the presence of a folded structure, we use the ϕ,ψ-dependent $d_{\alpha N(i, i + 1)}/d_{\alpha N(i, i)}$ intensity ratios (Fig. 5) as a guide for discriminating amongst the remaining possibilities, namely, the presence of extended, β-strand, or random coil states.[23,40,42,43] We find that S9–T8, I12–T11, and Q13–I12 sequence pairs possess NOE intensity ratios = 3.3, 6.2, and 3.1, all of which exceed the random coil value of 2.3 (Fig. 5).[23,40,42,43] However, the NOE ratio for the T11–G10 sequence pair was determined to be 1.7, which is lower than the random coil value. These values indicate that the S9–T8, I12–T11, and Q13–I12 regions exist in an extended conformational state,[23,40,42,43] consistent with our CD experiments which indicate that the GBP-1/14 polypeptide possesses some degree of non-random coil structure (Fig. 2). It is likely that the T11–G10 sequence pair adopts a coil-like conformation. *Based upon our NMR experiments, we conclude that the GBP-1/14 polypeptide repeat adopts an unfolded structure that is conformationally labile, with evidence of random coil structure within the MHGKTQA- sequence region, and extended structure/random coil preferences within the -TSGTIQS sequence segment.*

NMR studies of apo-GBP-1/42

Using the 14-mer polypeptide NMR assignments as a guide for the 42-mer polypeptide,[34] we were able to assign the corresponding overlapping spin systems as groupings (*e.g.*, M1, M15, M29, *etc.*) within the triple repeat (Fig. 4, Table 2). Due to chemical shift overlap, we were unable to quantitate $^3J_{NH–CH_\alpha}$ or NOEs for GBP-1/42. However, we observed that the majority of GBP-1/42 averaged ^1H NMR backbone chemical shifts exhibit little deviation (*i.e.*, within ±0.1 ppm) from the sequence-specific single repeat dataset (Fig. 3A, Tables 1 and 2), highly suggestive that both polypeptides adopt similar if not identical conformations at neutral pH. The
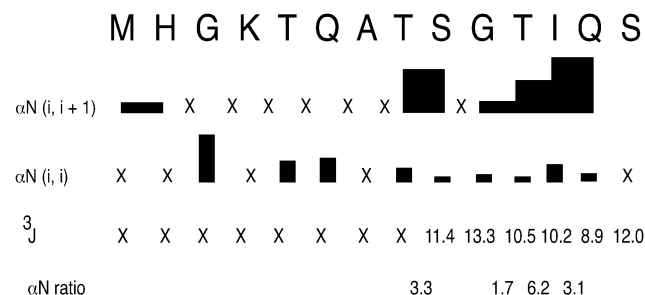

Fig. 5 Summary of NMR parameters for GBP-1/14 peptide in 100 µM Na_2HPO_4, pH 7.6, 90% H_2O/10% D_2O, 278 K. The summary includes interresidue sequential αN(i, i + 1) and intraresidue αN(i, i) NOEs, αN(i, i + 1)/αN(i, i) ratios (denoted here as αN ratio), $^3J_{NH–CH_\alpha}$ (^3J) couplings (Hz). "X" denotes residue values that were not quantitated due to chemical shift overlap or the presence of chemical/conformational exchange.

Table 2 500 MHz Proton chemical shifts (ppm, at 278 K) for GBP-1/42, 100 μM Na$_2$HPO$_4$, pH 7.6, 90% water/10% D$_2$O

Residue	NH	CH$_\alpha$	CH$_\beta$	CH$_\gamma$	CH$_\delta$	CH$_\varepsilon$	Ring H	Sidechain NH
M1/15/29	8.68	4.21	1.98	N/O				
H2/16/30	8.59	4.26	N/O				6.94, 7.99	N/O
G3/17/31	8.61	3.93						
K4/18/32	8.54	4.37	1.86	1.32	N/O	N/O		
T5/19/33	8.35	4.3	4.17	1.11				
Q6/20/34	8.63	4.24	1.90, 2.00	2.28				6.85, 7.40
A7/21/35	8.5	4.3	1.45					
T8/22/36	8.37	4.25	4.05	1.08				
S9/23/37	8.26	4.17	3.75					
G10/24/38	8.61	3.93						
T11/25/39	8.21	4.25	4.05	1.08				
I12/26/40	8.46	4.07	1.89	1.21, 1.50	0.93	0.8		
Q13/27/41	8.72	4.35	1.89, 2.02	2.29				6.87, 7.65
S14/28/42	8.49	4.37	3.81					

[a] Overlapping spin system assignments were obtained from analyses of GBP-1/42 z-PFG-TOCSY and NOESY experiments, with comparison to datasets obtained for GBP-1/14 (Table 1). Due to overlap, $^3J_{\mathrm{NH-CH}_\alpha}$ coupling constants were not determined for GBP-1/42. Proton chemical shifts are referenced from internal d$_4$-TSP. N/O = not observed.

NH–CHα NOESY spectra obtained for the GBP-1/42 protein exhibits similar spectral features ascribed to the single repeat (Fig. 4); furthermore, we note an absence of long-range backbone NOEs (i.e., > i + 1) and a lack of sequential $d_{\mathrm{NN}(i, \ i + 1)}$ NOEs for GBP-1/42 as well (data not shown). Interestingly, the GBP-1/42 NH–CHα NOESY fingerprint spectra indicates that not all of the expected residue-specific interresidue NOE connectivities are observable (Fig. 4). In particular, Q13/27/41–I12/26/40 and H2/16/30–M1/15/29 $d_{\alpha\mathrm{N}(i, \ i + 1)}$ NOEs are absent in the GBP-1/42 NOESY spectra, but are present in the GBP-1/14 ROESY spectra. From this, we infer the following: the GBP-1/42 polypeptide does not possess additional structural features which would have resulted in the appearance of additional NOE crosspeaks. Instead, the reduction in observable NOEs indicates that conformational exchange and/or motion-related relaxation effects within GBP-1/42 are leading to the cancellation of NOEs, a behavior which is consistent with an unfolded, conformationally labile polypeptide (Fig. 4).[23,40–44] *Thus, the GBP-1/42 appears to possess additional degrees of conformational lability that are not observed in the single repeat form, GBP-1/14 (Fig. 4).*

The NH–solvent exchange region of the GBP-1/42 NOESY spectra reveals that the majority of NH resonances experience exchange with the bulk solvent on the NMR timescale (milliseconds to seconds), indicating that there is little evidence for backbone hydrogen bonding within the GBP-1/42 polypeptide (Fig. 4).[23,45] The notable exceptions to this are the Q13/27/41 and S9/23/37 NH resonances, which exhibit no observable exchange with water, and, the G10/24/G38, Q6/20/34 NH resonances, which possess very weak NH–water NOE exchange peaks (Fig. 4; note arrows). Based upon previous studies, the lack of $d_{\mathrm{NN}(i, \ i + 1)}$ and $d_{\alpha\mathrm{N}(i, \ i + 1)}$ sequential NOEs, together with the absence of NH–solvent exchange NOEs, are not consistent with the presence of backbone hydrogen bonding, but may be attributable to solvent shielding arising from other factors, including partial folding, transient chain–chain association, and/or sidechain interaction.[23,44] *Combined with our CD data (Fig. 2), our ^1H NMR data supports the conclusion that both the GBP-1/14 and GBP-1/42 polypeptides adopt similar unfolded, labile conformations in solution.*

NMR studies of the 1 : 1 Au(III) : GBP-1/14 complex

To support the data obtained from our mass spectrometry and CD experiments, we utilized ^{1}H NMR spectroscopy to confirm the sequence location of Au(III) ion interaction within the -KTQATS- motif of GBP-1/14. A comparison of ^{1}H NMR chemical shifts, $^3J_{\mathrm{NH-CH}_\alpha}$ coupling constants (Tables 1 and 3) and PFG-ROESY spectra obtained for the apo-GBP-1/14 and 1 : 1 Au : GBP-1/14 samples (Fig. 6) reveals some interesting features. First, in accord with our CD findings, we note that Au(III) interactions with GBP-1/14 do not significantly alter the global conformation of the polypeptide, as evidenced by the absence of significant deviations (i.e., > 0.1 ppm) in backbone ^{1}H NMR chemical shifts for the 1 : 1 complex compared to the apo-GBP-1 polypeptide (Tables 1 and 3). This is in contrast to

Table 3 500 MHz Proton chemical shifts (ppm, at 278 K) for 1 : 1 Au(III) : GBP-1/14 complex, pH 7.6, 90% water/10% D$_2$O

Residue	NH	CH$_\alpha$	CH$_\beta$	CH$_\gamma$	CH$_\delta$	CH$_\varepsilon$	Ring H	Sidechain NH	$^3J_{\mathrm{NH-CH}_\alpha}$/Hz
M1	8.74	4.4	2.02, 2.13	2.39					—
H2	8.64	4.37	N/O			8.05		N/O	—
G3	8.64	3.92							12.9
K4	8.43	4.41	1.68, 1.80	1.44	N/O	2.99			—
T5	8.38	4.39	4.28	1.21					—
Q6	8.66	4.34	2.03, 2.13	2.38				6.86, 7.52	—
A7	8.45	4.39	1.36						—
T8	8.42	4.39	4.19	1.2					—
S9	8.27	4.27	3.84						11.1
G10	8.63	4.02							11.7
T11	8.22	4.34	4.15	1.12					9.6
I12	8.48	4.18	1.86	1.48	1.21	0.9			10.7
Q13	8.72	4.41	2.01	2.14	2.39			6.84, 7.60	9.9
S14	8.51	4.48	3.91						11.1

[a] The proton assignments were obtained from analyses of PFG-TOCSY and ROESY experiments. Diastereotopic protons are separated by commas. Proton chemical shifts are referenced from internal d$_4$-TSP. N/O = not observed. ^3J coupling constants were determined using z-PFG-TOCSY/ROESY experiments and spectral processing methods that permit coupling constant measurements from TOCSY and ROESY/NOESY spectra (estimated experimental error, ±0.9 Hz).[23] Dashed line indicates that coupling constants could not be determined due to crosspeak overlap.
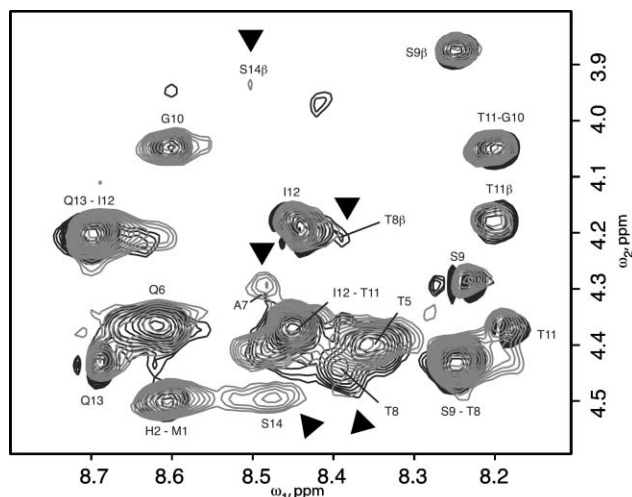
Fig. 6 Overlay of 200 ms mixing time PFG-ROESY NH–CHα fingerprint spectra obtained for apo-GBP-1/14 (black) and 1 : 1 Au : GBP-1/14 (gray), 278 K. Both spectra were acquired using identical acquisition parameters, sample volumes, and peptide concentrations. Acquisition parameters for GBP-1/14 included a relaxation delay of 1 s, spectral window = 5200 Hz, "hard" 90° = 8.7 μs, "hard" 180° = 17.4 μs; "soft" selective 180° = 3.2 ms; 256 transients per experiment were acquired; 2048 and 512 complex points were collected in t_1 and t_2, respectively. The carrier is centered on the water resonance. The t_m or mixing time for ROESY (compensated spinlock 180° pulse train) experiments was 200 ms. Z-Gradient parameters: $G_1 = 14$ G cm^{-1}, $G_2 = 6$ G cm^{-1}, each with a duration of 1 ms with 500 μs stabilization time. The hypercomplex phase-sensitive method was utilized for processing both 2-D spectra, with zero-filling in the ω_2 dimension. Proton chemical shifts are referenced from internal d$_4$-TSP. Black arrows indicate crosspeaks which exhibit intensity changes. Note that the intraresidue $d_{\alpha N(i,\ i)}$ NOE crosspeak for T8 is resolvable in the apo-peptide (black), but is not resolvable in the 1 : 1 Au : GBP-1/14 complex (gray).

the significant ^{1}H NMR chemical shift perturbation (*i.e.*, > 0.1 ppm) observed in Zn(II) finger polypeptides upon addition of Zn(II) or Zn(II)-analogues.[31–33] Similarly, with the exception of G3 and G10, we find that the $^3J_{NH-CH_\alpha}$ values obtained for the apo-GBP-1/14 and 1 : 1 GBP-1/14 : Au(III) complex are within experimental error (*i.e.*, ±0.9 Hz).[23,25] Additionally, the 1 : 1 GBP-1/14 : Au(III) complex does not possess sequential $d_{NN(i,\ i\ +\ 1)}$ NOEs, long-range $d_{NN(i,\ j)}$ backbone or $d_{sc(i,\ j)}$ sidechain NOEs, or evidence of backbone amide proton solvent exchange shielding (data not shown). These results indicate that the interaction of Au(III) does not induce secondary structure formation (*e.g.*, α-helix, β-hairpin) within the -KTQATS- containing tandem repeat.

Evidence of Au(III) interactions within the -KTQATS- sequence were noted *via* comparisons of the PFG-ROESY NH–CH$_\alpha$ fingerprint regions for the apo- and Au(III)-bound forms of GBP-1/14 (Fig. 6). Here, overlayed spectra reveal significant NOE crosspeak intensity changes for specific residues. In particular, we note (a) the disappearance of the intraresidue T8 NH–β-CH$_2$ crosspeak; (b) the disappearance and/or frequency shift of the T8 $d_{\alpha N(i,\ i)}$ crosspeak; (c) an increase in A7 intraresidue $d_{\alpha N(i,\ i)}$ crosspeak intensity; and (d) the appearance of intraresidue S14 $d_{\alpha N(i,\ i)}$ and NH–β-CH$_2$ crosspeaks (Fig. 6). The changes in intraresidue cross-relaxation for T8 and A7 are consistent with the presence of local conformational change in response to Au(III) interactions, and, is consistent with previous observations that the -KTQATS- sequence is a Au binding motif.[4] Hypothetically, the Q6 amide and T8–OH sidechain electron donor ligands may participate in interactions with Au(III), which, in turn, would affect the local conformation of the -QAT- sequence motif. Admittedly, the perturbation of S14 in the presence of Au(III) is not clearly understood at present, and, may possibly reflect non-specific

interaction of the C-terminal S14–OH and/or α-carboxylate groups with Au(III) ions in solution. However, Au(III) interactions within the -KTQATS- and the C-terminal end are consistent with the 1 : 2 GBP-1/14 : Au(III) adduct species detected by ion trap mass spectrometry (Fig. 1B). Thus, our NMR data indicate that the -QAT- sequence motif within the -KTQATS- domain is the locus of Au(III) interactions.

Discussion

In the initial report which described the genetic selection of gold binding or catalyzing polypeptides, it was hypothesized that these protein sequences were acting to bias accretion on the thin edges of the Au crystals.[4] Since it was noted that Au crystals of the same shape are formed under acidic conditions, the simplest model for the action of the gold binding sequences was proposed to be the alteration of the local chemical environment, for example, by regulating the pH.[4] Although the specific mechanism of protein-catalyzed Au crystal formation is still not known, our studies support the hypothesis that GBP-1 does not catalyze Au crystal formation *via* a templating mechanism, and point to the possibility that the unfolded polypeptide state must play a role in Au crystal formation. Specifically, our current study demonstrates the following: (1) the -KTQATS- sequence, and the -QAT- motif in particular, is a Au(III) interaction site and thus is most likely involved in the Au(III) → Au crystal catalysis process; (2) the gold binding 14-AA tandem repeat adopts a random coil extended structure conformation [*i.e.*, (MHGKTQA)$_{random coil}$–(TSGTIQS)$_{extended}$], and the 42 AA GBP-1 protein exists in an unfolded, unstable conformational state that most likely exists as some combination of random coil and extended structure. Note that this finding is in contrast to the hypothetical β-hairpin arrangement for GBP-1 proposed in earlier modeling studies;[2b] (3) in the presence and absence of Au(III), we observe that the conformations of -KTQATS- and the GBP-1 protein persist in an unfolded, labile state, which is inconsistent with the typical rigid-like organization associated with a molecular template[18–22] or with other structured metalloproteins.[31–33] Thus, based upon our findings, the GBP-1 protein and the -KTQATS- sequence are interactive with Au(III) ions and most likely exploit some type of non-templating molecular mechanism(s) to achieve Au crystal formation.

A number of comments should be made at this point. First, it is not clear what significance, if any, the conformational equilibria shift observed for GBP-1 in the presence of Au(III) (Fig. 2) has with regard to Au crystal formation. Second, since the Au(III) binding affinity of GBP-1 or -KTQATS- cannot be ascertained from our study, it is not clear whether the GBP-1 tandem sequence interacts strongly or weakly with Au(III) ions in solution, or, how the magnitude of these interactions might influence Au crystal catalysis. Third, although we now understand the solution-state structure of GBP-1, we do not know whether the Au crystal-adsorbed GBP-1 protein adopts a conformation similar to or different from that described for the solution-state. The reader should note that recent studies have demonstrated that solution-state conformations of polypeptides play an important role in polypeptide interfacial recognition.[46–48] Thus, it is likely that unfolded, open conformations play a key role in the strong interaction of these polypeptides with exposed interfaces,[46] and may partially explain GBP-1 interactions with exposed Au metal interfaces.[2] Additional experiments in solution and in the solid state are currently in progress to address these issues.

If the Au(III) → Au (crystal) acid-catalyzed transformation process takes place in the presence of an unfolded, conformationally labile polypeptide ensemble, then the next question to be addressed is how unfolded polypeptides can accomplish this task. Some plausible answers to this question might be

provided by two recent studies. The first, that of bismuth sulfide Bi_2S_3 nanorod formation in the presence of the bioreagent, glutathione,[49] reveals that a simple polypeptide such as glutathione, which lacks the hierarchical structure of a folded protein, can control Bi_2S_3 nanomaterial formation by acting as a sulfur donor and as an assembling agent.[49] The second study, that of the stabilization and transformation of amorphous inorganic biominerals in the presence of polyelectrolytes,[50] suggests that a combination of solution- and solid-state mechanisms are at work in calcium phosphate crystal growth, and, that these mechanisms involve interactions between unstructured, reactive polyelectrolyte polypeptides, the inorganic solid phase, and, free ions in solution.[50] What seems to be required in either case are accessible reactive groups and some form of thermodynamic or entropic stabilization. Based upon these observations, we hypothesize that the formation of Au crystals in the presence of GBP-1 could be likewise directed by a combination of Au crystal–polypeptide *and* Au(III)–polypeptide interactions. For example, the conformational instability of unfolded GBP-1 could act as a driving force for polypeptide adhesion with forming Au clusters, whereas the unfolded nature of the -KTQATS-sequence permits interaction with Au(III) and accessibility of proton donors (*e.g.*, Gln, Thr, Ser, His, Lys) which may participate in the proposed acid-catalyzed or pH-mediated formation of Au crystals.[4] Obviously, there may be other explanations or plausible models which fit the data, and additional experimentation will be required to determine how the open, unfolded, Au(III) interactive structure of GBP-1 directs Au crystal formation in solution and interacts with exposed Au interfaces.

Acknowledgements

References

1 M. Sarikaya, *Proc. Natl. Acad. Sci. U. S. A.*, 1999, **96**, 14183–14185.
2 (*a*) M. Sarikaya, C. Tamerler, A. K.-Y. Jen, K. S. Schulten and F. Baneyx, *Nature Mater.*, 2003, **2**, 577–585; (*b*) R. Braun, M. Sarikaya and K. S. Schulten, *J. Biomater. Sci.*, 2002, **13**, 747–758.
3 (*a*) S. Brown, *Nature Biotechnol.*, 1997, **15**, 269–272; (*b*) S. Brown, *Proc. Natl Acad. Sci. U. S. A.*, 1992, **89**, 8651–8655.
4 S. Brown, M. Sarikaya and E. Johnson, *J. Mol. Biol.*, 2000, **299**, 725–732.
5 M. Sarikaya, H. Fong, D. Heidel and R. Humbert, *Mater. Sci. Forum*, 1999, **293**, 83–87.
6 R. R. Naik, L. Brott, S. J. Carlson and M. O. Stone, *J. Nanosci. Nanotechnol.*, 2002, **2**, 1–6.
7 K. Kiargaard, J. K. Sorensen, M. A. Schembri and P. Klemm, *Appl. Env. Microbiol.*, 2000, **66**, 10–14.
8 D. J. H. Gaskin, K. Starck and E. N. Vulfson, *Biotechnol. Lett.*, 2000, **22**, 1211–1216.
9 S. R. Whaley, D. S. English, E. L. Hu, P. F. Barbara and A. M. Belcher, *Nature*, 2000, **405**, 665–668.
10 W. S. Lee, C. Mao, C. E. Flynn and A. M. Belcher, *Science*, 2002, **296**, 892–895.
11 I. Sarashina and K. Endo, *Am. Mineral.*, 1998, **83**, 1510–1515.
12 L. Bedouet, M. J. Schuller, F. Marin, C. Milet, E. Lopez and M. Giraud, *Comp. Biochem. Physiol., B: Biochem. Mol. Biol.*, 2001, **128**, 389–400.
13 M. Kono, N. Hayashi and T. Samata, *Biochem. Biophys. Res. Commun.*, 2000, **269**, 213–218.
14 T. Samata, N. Hayashi, M. Kono, K. Hasegawa, C. Horita and S. Akera, *FEBS Lett.*, 1999, **462**, 225–229.
15 I. M. Weiss, S. Kaufmann, K. Mann and M. Fritz, *Biochem. Biophys. Res. Commun.*, 2000, **267**, 17–21.
16 I. W. Kim, E. DiMasi and J. S. Evans, *Cryst. Growth Des.*, submitted.
17 M. Michenfelder, G. Fu, C. Lawrence, J. C. Weaver, B. A. Wustman, L. Taranto, J. S. Evans and D. E. Morse, *Biopolymers*, 2003, **70**, 522–533.
18 A. V. Kajava and S. E. Lindow, *J. Mol. Biol*, 1993, **276**, 709–717.
19 P. V. Braun, P. Osenar, V. Tohver, S. B. Kennedy and S. I. Stupp, *J. Am. Chem. Soc.*, 1999, **121**, 7302–7309.
20 P. A. Ngankam, Ph. Lavalle, J. C. Voegel, L. Szyk, G. Decher, P. Schaaf and F. J. G. Cuisinier, *J. Am. Chem. Soc.*, 2000, **122**, 8998–9005.
21 J. J. M. Donners, J. M. R. Nolte and N. A. J. M. Sommerdijk, *J. Am. Chem. Soc.*, 2002, **124**, 9700–9701.
22 Y.-J. Han and J. Aizenberg, *J. Am. Chem. Soc.*, 2003, **125**, 4032–4033.
23 B. A. Wustman, J. C. Weaver, D. E. Morse and J. S. Evans, *Langmuir*, 2003, **19**, 9373–9381.
24 G. Xu and J. S. Evans, *J. Magn. Reson., Ser. B*, 1996, **111**, 183–185.
25 Y. Wang, A. M. Nip and D. S. Wishart, *J. Biomol. NMR*, 1997, **10**, 372–279.
26 S. J. Shields, B. K. Bluhm and D. H. Russell, *Int. J. Mass Spectrom.*, 1999, **182**(183), 185–191.
27 K. L. C. Wong and T. W. D. Chan, *Rapid Commun. Mass Spectrom.*, 1997, **11**, 513–516.
28 A. Perczel, M. Hollosi, P. Sandor and G. D. Fasman, *Int. J. Pept. Protein Res.*, 1993, **41**, 223–236.
29 N. Sreerama and R. W. Woody, *Biochemistry*, 1994, **88**, 10022–10025.
30 M. Ramirez-Alvarado, F. J. Blanco, H. Niemann and L. Serrano, *J. Mol. Biol.*, 1997, **273**, 898–912.
31 N. D. Clarke and J. M. Berg, *Science*, 1998, **282**, 2018–2022.
32 H. Berkovits and J. M. Berg, *Biochemistry*, 1999, **38**, 16826–16830.
33 M. Schmiedeskamp and R. E. Klevit, *Biochemistry*, 1997, **36**, 14003–14011.
34 B. A. Wustman, R. Santos, B. Zhang and J. S. Evans, *Biopolymers*, 2002.
35 D. S. Wishart, B. D. Sykes and F. M. Richards, *J. Mol. Biol.*, 1991, **222**, 311–333.
36 D. S. Wishart, C. G. Bigam, J. Yao, F. Abildgaard, H. J. Dyson, E. Oldfield, J. L. Markley and B. D. Sykes, *J. Biomol. NMR*, 1995, **6**, 135–140.
37 D. S. Wishart, C. G. Bigam, A. Holm, R. S. Hodges and B. D. Sykes, *J. Biomol. NMR*, 1995, **5**, 67–81.
38 L. Serrano, *J. Mol. Biol.*, 1995, **254**, 322–333.
39 L. J. Smith, K. A. Bolin, H. Schwalbe, M. W. MacArthur, J. M. Thornton and C. M. Dobson, *J. Mol. Biol.*, 1996, **255**, 494–506.
40 K. Ma, L. S. Kan and S. Wang, *Biochemistry*, 2001, **40**, 3427–3438.
41 A. Pardi, M. Biliter and K. Wuthrich, *J. Mol. Biol.*, 1984, **180**, 741–751.
42 D. Neuhaus and M. P. Williamson, in *The Nuclear Overhauser Effect in Structural and Conformational Analysis*, Wiley-VCH, New York, NY, 2000, p. 498.
43 K. M. Fiebig, H. Schwalbe, M. Buck, L. J. Smith and C. M. Dobson, *J. Phys. Chem.*, 1996, **100**, 2661–2666.
44 D. Neri, M. Billiter, G. Wider and K. Wuthrich, *Science*, 1992, **257**, 1559–1563.
45 N. H. Andersen, J. W. Neidigh, S. M. Harris, G. M. Lee, Z. Liu and H. Tong, *J. Am. Chem. Soc.*, 1997, **119**, 8547–8561.
46 J. S. Evans, *Curr. Opin. Colloid Interface Sci.*, 2003, **8**, 48–54.
47 Q. Q. Hoang, F. Sicheri, A. J. Howard and D. S. C. Yang, *Nature*, 2003, **425**, 977–980.
48 M. C. Loewen, W. Gronwald, F. D. Sonnichsen, B. D. Sykes and P. L. Davies, *Biochemistry*, 1998, **37**, 17745–17753.
49 Q. Lu, F. Gao and S. Komarneni, *J. Am. Chem Soc.*, 2004, **126**, 54–55.
50 P. B.-Y. Ofir, R. G. Lippman and H. F.-M. Garti, *Cryst. Growth Des.*, 2004, **4**, 177–183.